THE ASTROPHYSICAL JOURNAL, 446:583–593, 1995 June 20

EVIDENCE FOR AN ON-GOING CLUSTER/GROUP MERGER IN ABELL 2255

JACK O. BURNS, KURT ROETTIGER, AND JASON PINKNEY
Department of Astronomy, New Mexico State University, Las Cruces, NM 88003;
jburns@nmsu.edu; kroettig@nmsu.edu; jpinkney@nmsu.edu

RICK A. PERLEY AND FRAZER N. OWEN
National Radio Astronomy Observatory,[1] P.O. Box O, Socorro, NM 87801;
rperley@aoc.nrao.edu; fowen@aoc.nrao.edu

AND

WOLFGANG VOGES
Max-Planck-Institut für Extraterrestrische Physik, Postfach 1603, D-85740, Garching bei München, Germany;
whv@mpe.dnet.nasa.gov
Received 1994 July 20; accepted 1994 December 27

ABSTRACT

We report on new X-ray, radio, and optical observations of the rich cluster Abell 2255. These new observations have revealed interesting and unusual characteristics at each wavelength band that are inconsistent with a simple, relaxed cluster. *ROSAT* all-sky survey (RASS) and CCD *r*-band images show that the cluster X-ray centroid does not coincide with any bright cluster galaxies or subgroup of galaxies. Furthermore, RASS spectra indicate cool (2 keV) gas within 5′ of the X-ray centroid whereas *Einstein* MPC spectra indicate a temperature of 7.3 keV for the cluster as a whole. At 1240 km s^{-1}, A2255 has one of the highest known Abell cluster velocity dispersions; also, the two brightest cluster galaxies are separated by an unusually large 2635 km s^{-1}. Our new VLA 20 cm imaging has revealed a distorted, off-center, steep-spectrum diffuse radio source, previously labeled a radio halo, and a peculiar ridge of radio emission $\approx$0.6 Mpc north of the X-ray centroid. We believe that these cluster properties can be understood if A2255 is in the process of merging with a galaxy group. We present a numerical Hydro/*N*-body simulation of such a merger which nicely reproduces the X-ray and galaxy velocity properties, and the merger has sufficient energy to power the diffuse cluster radio emission.

Subject headings: galaxies: clusters: individual (A2255) — galaxies: interactions — intergalactic medium — radio continuum: galaxies — X-rays: galaxies

1. INTRODUCTION

Abell 2255 is an interesting and unusual galaxy cluster. It is richer than 95% of clusters in Abell's (1958) complete sample (richness class 2). Zwicky & Herzog (1968) identified this region as containing a 2° diameter cluster with 345 member galaxies. A2255 is classified as a Bautz & Morgan (1970) type II-III cluster with a redshift of 0.080 (Abell, Corwin, & Olowin 1989) (distance = 302.4 Mpc and 1″ = 1.36 kpc for H_0 = 75 km s^{-1} Mpc^{-1} and q_0 = 0.5 used throughout this paper). There are two relatively bright ($m_p \approx 17$) elliptical galaxies near the apparent cluster center. Zwicky (1971) also took special note of this cluster as one containing a number of red "compact" galaxies.

The interpretation of the galaxy dynamics in A2255 has been controversial. Using velocities for 15 galaxies, Tarenghi & Scott (1976) suggested that the apparent two-peaked distribution of redshifts indicated that A2255 was actually two superposed clusters. However, after adding another 18 galaxy spectra, Stauffer et al. (1979) found a more continuous distribution of galaxy redshifts which they interpreted as evidence for a single cluster with an unusually large radial velocity dispersion of $\approx$1200 km s^{-1}.

A2255 is one of only a few rich clusters that is reported to have an extensive cluster radio halo (Jaffe & Rudnick 1979; Hanisch 1982). A WSRT image of A2255 at 610 MHz (Harris Kapahi, & Ekers 1980) shows evidence for $\approx$0.5 Mpc diameter diffuse central radio emission with a very steep spectrum. After subtracting compact and head-tail sources, Harris et al. find that the remaining diffuse radio emission in A2255 has $\alpha = 1.7$ (where $S_\nu \propto \nu^{-\alpha}$). This cluster also has an unusually large number (10) of individual radio galaxies (Harris et al. 1980). Five of these radio galaxies have head-tail radio morphologies. Assuming that the extended radio emission is thermal pressure confined, Hintzen & Scott (1980) inferred the presence of cluster gas out to 10–20 core radii from the cluster center ($\lesssim$3.5 Mpc).

The first reliable X-ray detection of A2255 was from *HEAO 1* with an apparent 2–10 keV luminosity of 2×10^{44} ergs s^{-1} (Hintzen & Scott 1980; Kowalski et al. 1984). Forman & Jones (1982) and Jones & Forman (1984) discussed the first X-ray imaging observations of A2255 using the *Einstein Observatory* with an effective resolution of FWHM = 1.′7 (139 kpc). They measured a 0.5–3.0 keV luminosity of 6.2×10^{43} ergs s^{-1} out to a radius of 0.33 Mpc. Jones & Forman found that A2255 has one of the largest X-ray core radii ($\approx$0.4 Mpc) in their sample of 46 clusters. Further analysis of the X-ray surface brightness by McMillan, Kowalski, & Ulmer (1989) and Rhee, van Haarlen, & Katgert (1992) revealed that the X-ray emission for this cluster is relatively circular. Using a deprojection of the *Einstein* surface brightness profile, Stewart et al. (1984) inferred a central cooling time of 6.6×10^{10} yr and, therefore, concluded that A2255 does not have a cooling inflow. The lack of a cluster cooling flow in such a rich cluster is unusual since Edge, Stewart, & Fabian (1992) find evidence for such flows in

[1] The National Radio Astronomy Observatory is operated by Associated Universities, Inc., under cooperative agreement with the National Science Foundation.

75%–90% of their X-ray bright sample. David et al. (1993) recently reported an average cluster temperature of $7.3^{+1.7}_{-1.1}$ keV (1 σ errors) for A2255 using an *Einstein* MPC spectrum. Finally, Forman & Jones (1982) classified A2255, along with the Coma cluster, as the prototype of a class of "relaxed," evolved cluster without a dominant galaxy (nXD) which has a high X-ray luminosity, a hot ICM, a high-velocity dispersion, and no central cooling flow.

We are interested in A2255 as part of a study of the multi-wavelength properties of clusters with radio halos (Burns et al. 1992, 1994b). In this paper, we present new X-ray, optical, and radio data on A2255 in an effort to understand the origin of the unusual cluster properties. In § 2, we discuss *ROSAT* X-ray, CCD optical, and VLA radio images of A2255. A new analysis of the galaxy velocity distribution is also presented. In § 3, we compare the X-ray, radio, and optical properties of A2255 with other clusters. In § 4, we advance the hypothesis that A2255 is a cluster which is undergoing a merger. The results of numerical Hydro/*N*-body simulation are presented to support this idea. In § 5, we summarize our results and present conclusions.

2. NEW OBSERVATIONS AND DATA ANALYSIS

2.1. *ROSAT Imaging and Spectral Data*

Because of its high ecliptic latitude of 84°.5, A2255 was observed repeatedly by the *ROSAT* satellite during its initial 6 months all-sky survey (hereafter RASS; see, e.g., Trümper 1993; Voges 1992). As a result, $\approx$3500 s of total integration was obtained by the PSPC, thus producing one of deepest X-ray images of any cluster in the RASS. We merged together all the individual scans of A2255 to produce the X-ray image, shown overlaid onto an optical CCD image (see § 2.2), in Figure 1. This RASS map is for the energy band 0.51–2.01 keV. It was flat-fielded using an exposure map constructed from the integration times for the summed scans. The image in Figure 1 was smoothed with a circular Gaussian of 51″ FWHM (69.4 kpc).

We compared the positions, luminosities, and structures of the *Einstein* IPC image of A2255 from the CfA CD ROM (Harris et al. 1990), which has 1′.7 resolution, to our new, higher resolution image in Figure 1. First, the X-ray centroid positions were found to agree within 27″. This matches well with the expected position errors for the RASS (Voges 1992). Second, we measured a background-corrected count rate of 0.34 counts s^{-1} within the above bandwidth out to a radius of 0.33 Mpc on the RASS image. Using an H I column density of 2.5×10^{20} cm^{-2} (Stark et al. 1992) to correct for photoelectric absorption, the corresponding X-ray flux is 4.9×10^{-12} ergs cm^{-2} s^{-1} and the 0.5–2.0 keV luminosity is 5.9×10^{43} ergs s^{-1}. Given the difference in bandwidths and uncertainties in the measurements, this RASS luminosity is in good agreement with the *Einstein* observation (Jones & Forman 1984). Finally, we overlaid the *ROSAT* and *Einstein* images and also found good correspondence in the basic structures. Both images show that the X-ray surface brightness of A2255 beyond 1′ from the X-ray peak is elongated along a position angle of $\approx$80°. However, the higher resolution RASS image reveals a more compact, central feature than that seen on the *Einstein* image. Surprisingly, this X-ray peak is $\approx$2′ away from the brightest cluster galaxy (well in excess of the astrometric errors in either the RASS or CCD images) and does not obviously coincide with any prominent cluster galaxy or grouping of galaxies. A similar offset between the X-ray and optical centroids in A754 was reported by Ulmer, Wirth, & Kowalski (1992).

After subtracting an average X-ray background of 2.6×10^{-4} counts s^{-1} arcmin^{-2} from the RASS image, we produced an X-ray surface brightness profile for A2255 using

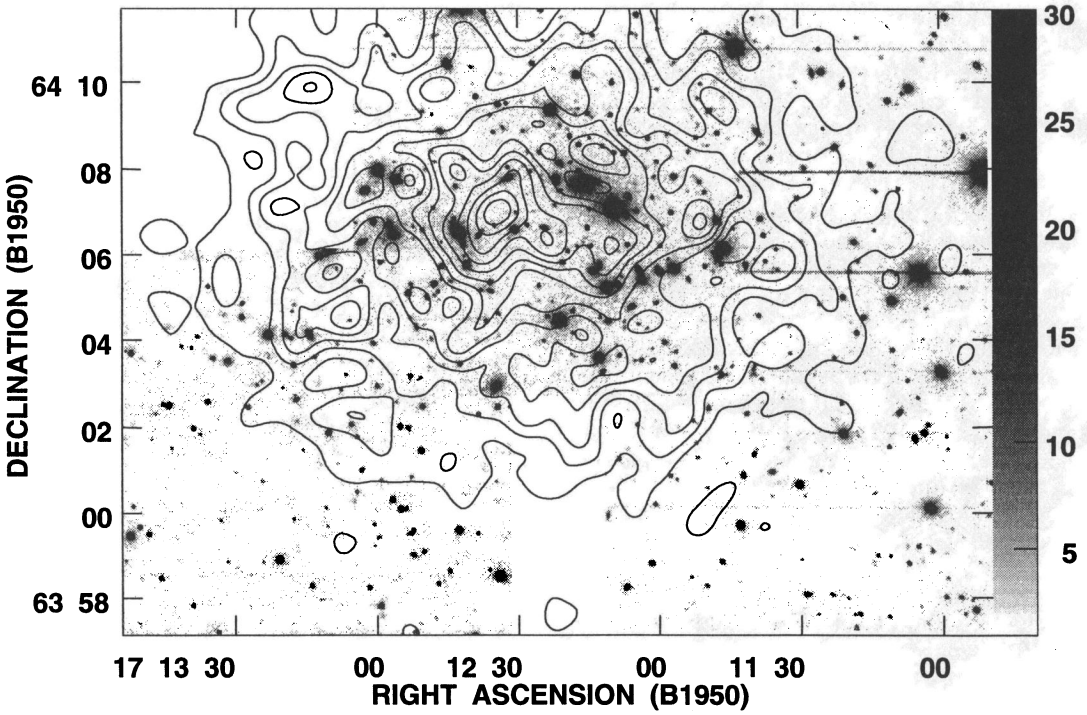

FIG. 1.—Contours of 0.5–2.0 keV X-ray emission from the *ROSAT* all-sky survey superposed onto a gray-scale *r*-band CCD image of A2255. X-ray image has been convolved with a 51″ FWHM Gaussian. Contour levels are 10, 15, 20, 25, 30, 35, 40, 45, 50, 55, 60, and 65 $\times$ 10^{-5} counts s^{-1} (15″ $\times$ 15″ pixel)$^{-1}$.

circular annuli of width 29″ (not shown). We then attempted to fit isothermal King models (e.g., Sarazin 1986), $S = S_0[1 + (r/r_c)^2]^{-3\beta+1/2}$, to the profile. We found this profile to be complex and not easily fitted by a single King model. If we fit the X-ray profile only between 1.′7 and 6.′7 (135–547 kpc) from the cluster peak, we find a core radius (r_c) of 362″ ± 68″ (492 kpc) and $\beta = 0.70 \pm 0.26$ (1 σ errors), in good agreement with that published by Jones & Forman (1984) from *Einstein* IPC data. On the other hand, if we include the significant X-ray emission in the profile out to 12′ (979 kpc), the best-fit values are $r_c = 549'' \pm 31''$ (747 kpc) and $\beta = 1.25 \pm 0.18$. This difference is caused by the "hump" in the X-ray surface brightness profile beyond 7′. For either King model fit, there is an ≈45% excess of X-ray emission when extrapolating the King model fit into the center of the cluster, corresponding to a small luminosity excess of $\approx 2 \times 10^{42}$ ergs s^{-1}.

This profile was then deprojected into distributions of gas density (Fig. 2*a*) and temperature (Fig. 2*b*) using a technique similar to that described by Arnaud (1988). In brief, this deprojection method utilizes a Raymond-Smith (1977) thermal spectrum with the gas assumed to be in quasi-hydrostatic equilibrium within spherical shells. The outer potential is constrained to follow a King model with the above X-ray parameters. Our best deprojection utilized an outer temperature of 8 keV and a galaxy radial velocity dispersion (σ_R) of 1000 km s^{-1}. This lower than observed (see § 2.3) value of σ_R was needed to reproduce the spectroscopically determined X-ray temperature distribution described below. Because the X-ray emissivity observed in the *ROSAT* band is $\propto n^2 T^{1/2}(e^{-0.5/kT} - e^{-2.0/kT})$, the deprojected density is well constrained but the temperature is poorly determined.

There were sufficient X-ray counts in the A2255 RASS database to fit a thermal model to the spectrum and to measure the temperature at the core of the cluster. Counts within a circular aperture of radius 5′ (≈400 kpc) centered on the X-ray peak were used to construct the spectrum. The background was determined from an annulus of width 10′ around the circular aperture. Using the EXSAS software package within MIDAS, the spectrum was fitted between 0.2 and 2.0 keV using a Raymond-Smith (1977) model with an assumed 30% of solar heavy metal abundance, typical for clusters of galaxies (Butcher & Stewart 1991). The spectral channels were first

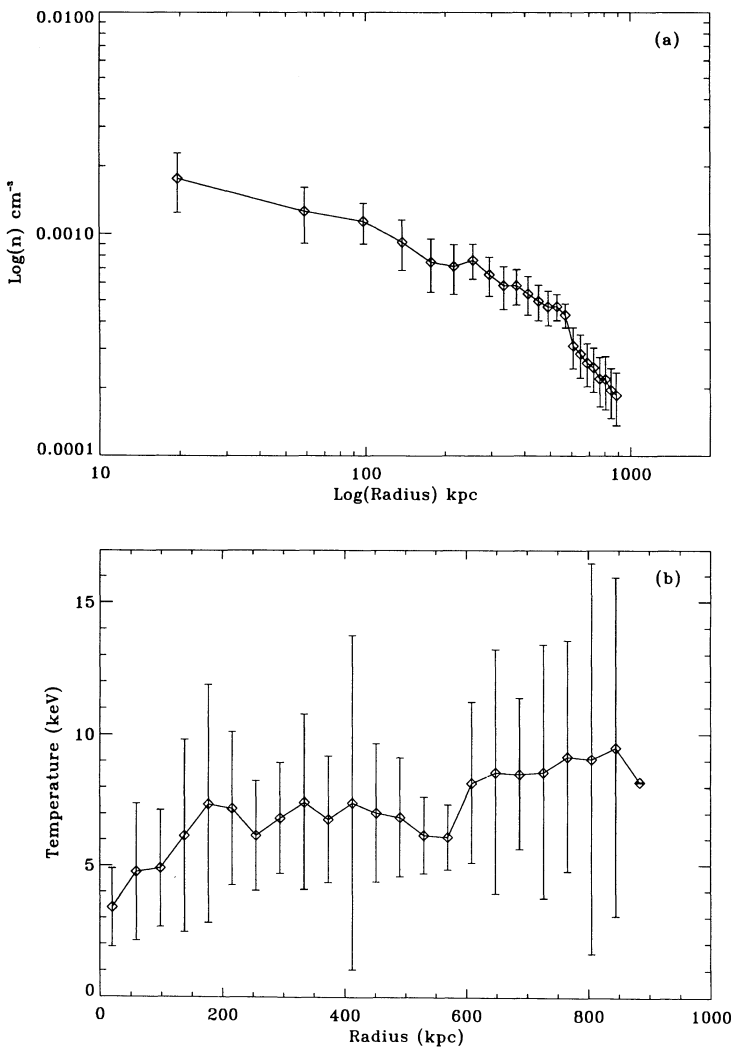

FIG. 2.—(*a*) Deprojected gas density distribution from the X-ray surface brightness profile. (*b*) Deprojected gas temperature distribution from the X-ray surface brightness profile.

averaged into bins with S/N $\geq$ 3 and then the thermal model was fitted to the spectrum. Two free parameters, temperature and N_H, were adjusted until the best χ^2 was achieved. The spectrum and the thermal model are shown in Figure 3. The results of these fits indicate a core temperature of $1.9^{+2.3}_{-0.4}$ keV, $N_H = 2.4^{+0.7}_{-0.6} \times 10^{20}$ atoms cm^{-2} (90% confidence errors), and a reduced χ^2 of 0.99. Our fitted value of N_H agrees well with that of Stark et al. (1992) from 21 cm observations. However, given the errors in the *ROSAT* and the *Einstein* MPC spectral fits, the central temperature in A2255 is different from the average cluster temperature measured by David et al. (1993) on the greater than 90% level. This suggests the possible presence of cool gas in the cluster core, the nature of which will be discussed in § 4.

2.2. *CCD Imaging Observations*

In Figure 1, and Figure 5*a* below, an optical *r*-band (Thuan & Gunn 1976) image of A2255 with a field of view of 1.67 × 1.21 Mpc is displayed. This image is the result of mosaicing four overlapping CCD frames taken with the NMSU Blue Mesa Observatory 0.61 m telescope in 1993 May and June using a Tektronics 1024 × 1024 chip. The central frame had a 10 minute exposure whereas the other three frames were 5 minutes each. These data were collected during non-photometric conditions so we have not attempted to extract magnitudes from the images.

Bias subtraction, flat-fielding, and cosmic-ray removal were performed in the usual fashion using the NOAO IRAF package. A median of 10 *r*-band images collected during one night were used for flat-fielding. The four A2255 images were then aligned using star centroid positions with mosaicing software in IRAF. The star positions were calibrated using the Space Telescope Guide Star Catalog. The final RMS scatter in positions across the field is 2.″9 in right ascension and 1.″3 in declination.

As described in the previous section, there are no obvious cluster galaxies associated with the X-ray peak in A2255. In addition, we note that the northern bright elliptical galaxy (see position below) shows isophotal distortions on the CCD image, suggestive of recent tidal interaction.

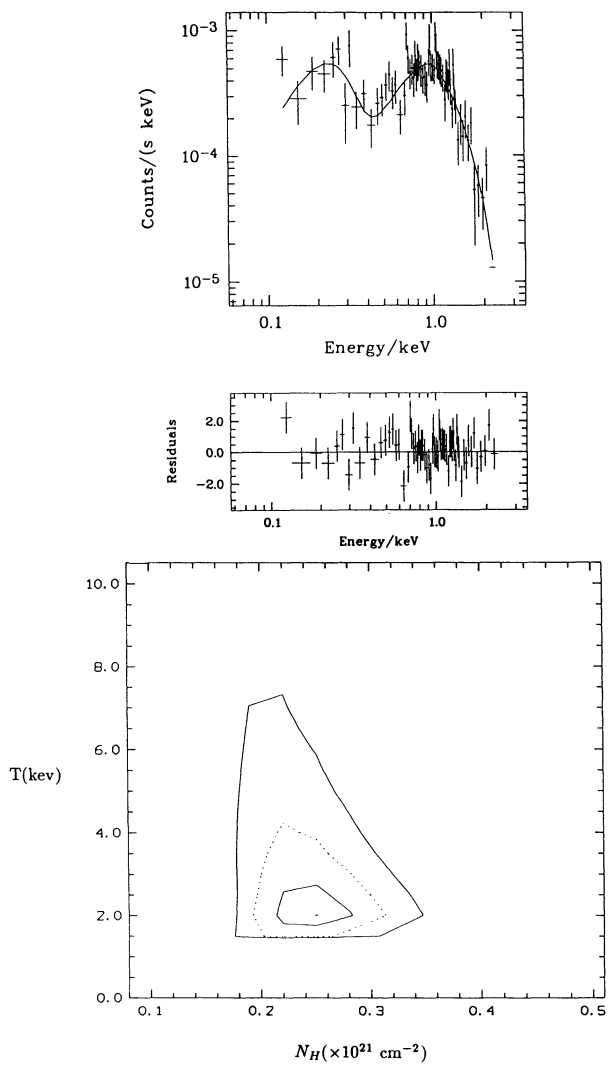

FIG. 3.—Spectral fit to the RASS data for a circle of 5′ radius centered on the X-ray peak. Curve in the top panel is the best-fit Raymond-Smith model, with the parameters given in Table 1, folded into the PSPC detector response. The middle panel illustrates the residuals of the fit to the data. The bottom panel shows the confidence limits on the two fitted parameters with contour levels of 68%, 90%, and 99%.

2.3. *Galaxy Velocities*

The distribution of measured galaxy velocities for A2255 assembled from Tarenghi & Scott (1976), Stauffer et al. (1979), and Hintzen & Scott (1980) is shown in Figure 4. The distribution is broad with a possible tail toward lower velocities. This peculiar distribution has led to some difference of opinions in the literature on the nature of this cluster, as discussed in § 1. The two brightest ellipticals in Figure 1 are separated by 2635 km s^{-1} in radial velocity with the northern galaxy ($\alpha = 17^h12^m15^s.9$; $\delta = 64°07'42''$; $cz = 24{,}706$) closest to the cluster velocity centroid. The seven galaxies with $cz < 23{,}000$ km s^{-1} are spread uniformly across the cluster as projected onto the sky plane.

To investigate this velocity distribution more quantitatively, we used the *ROSTAT* software package written by Beers et al. (1990) on the 39 measured redshifts within the velocity interval in Figure 4. *ROSTAT* uses non-Gaussian statistics to measure quantities analogous to the velocity mean (called biweight location) and standard deviation (called biweight scale). It characterizes the shape of the velocity distribution using resistant estimators that are less sensitive to velocity interlopers. Estimates of the confidence intervals for the biweight location and scale were obtained by application of the bias-corrected accelerated bootstrap procedures, using 1000 bootstrap samples as described by Beers et al. (1990). The resulting parameters for this cluster are listed in Table 1. The biweight location, C_{BI}, of the cluster is also indicated on Figure 4. The

TABLE 1

CLUSTER DYNAMICS FOR A2255

Mean	Location	Dispersion	Scale
24,173.....	$24{,}330^{+203}_{-265}$	1208	1240^{+203}_{-129}

NOTES.—Columns have units of km s^{-1}. The mean and biweight location (analogous to mean; see text) estimates are heliocentrically corrected. Dispersion, biweight scale (analogous to dispersion), and errors have cosmological and velocity-error corrections. Sixty-eight percent confidence intervals are used for the errors.

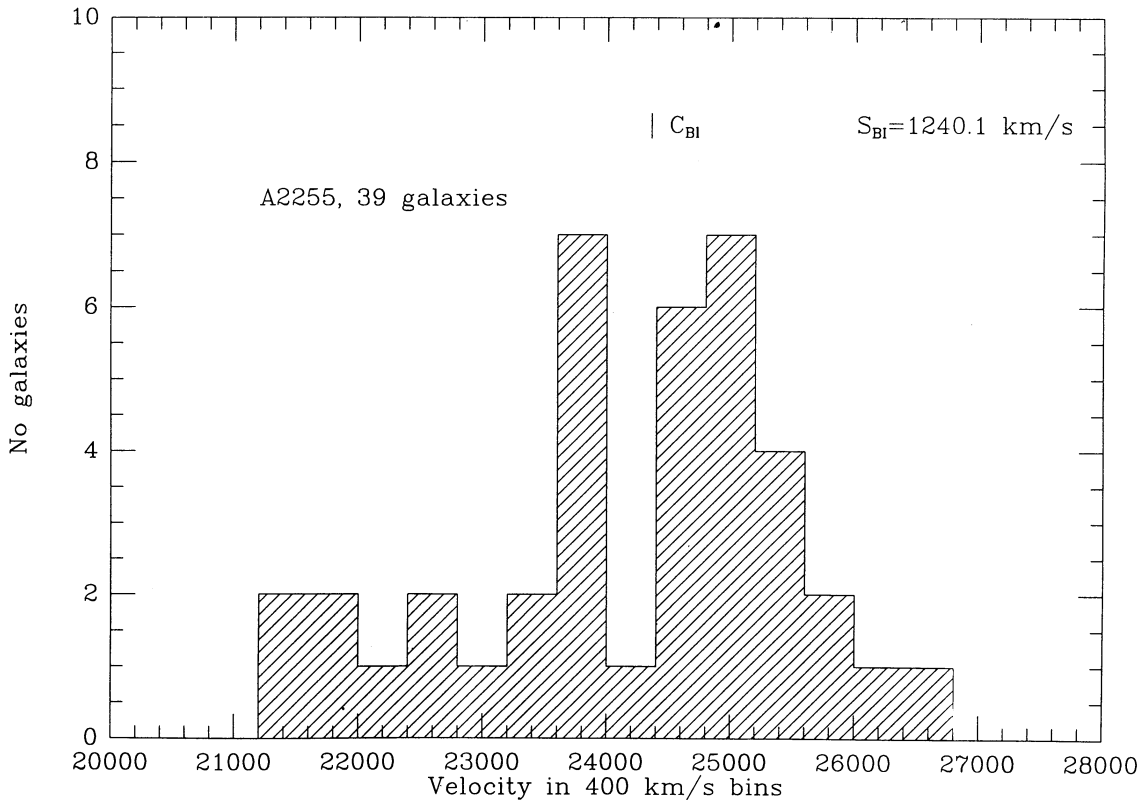

FIG. 4.—Distribution of measured galaxy velocities for A2255. C_{BI} is the biweight location.

A2255 velocity distribution has an unusually large biweight scale of 1240 km s^{-1}. The measurements in Table 1 include proper cosmological corrections (e.g., Danese, DeZotti, & di Tullio 1980), assuming 100 km s^{-1} errors on the velocities.

In addition, we applied 15 normality tests to the distribution in Figure 4. None of these tests indicate that the velocity distribution is significantly non-Gaussian (i.e., none show $<19\%$ probability of being drawn from a normal distribution). This distribution has neither an excessively long tail (kurtosis) nor asymmetry (skewness). Similar results were found using the reportedly more conservative tail index and asymmetry index from Bird & Beers (1993). We also used the Dressler-Shectman (1988) δ-test for substructure which compares the local velocity mean and dispersion with the global mean and dispersion. Once again, no significant substructure was found. However, it is important to keep in mind the relatively small number of galaxy redshifts that are available in the literature for A2255.

2.4. *VLA 20 Centimeter Imaging*

A2255 was observed in the VLA C (1993 November 14) and D (1992 April 23) configurations at 1.4 GHz with a bandwidth of 50 MHz over a period of 10 hr. This produced excellent (u, v) coverage. Standard amplitude and phase calibrations were applied to the data from each configuration, followed by mapping, cleaning, and self-calibration (see, e.g., Perley, Schwab, & Bridle 1989) using the NRAO AIPS package. Finally, the visibility data from the two configurations were combined and additional self-calibration and mapping were performed. The final cleaned map was convolved with a circular Gaussian of FWHM 50″, effectively the same as the RASS image. It was also corrected for primary beam attenuation. The RMS noise on this image is 0.13 mJy $beam^{-1}$ (0.19 mJy $arcmin^{-2}$).

In Figure 5*a*, we present an overlay of the central portion of the VLA map onto the optical CCD image. In Figure 5*b*, we overlay the same VLA map onto a gray-scale image from the RASS database. Several interesting points can be made from these comparisons. First, the purported, steep-spectrum radio "halo" consists primarily of diffuse emission to the NW of the X-ray centroid. As first noted by Harris et al. (1980), this "halo" may be related to the extended emission coming from individual head-tail radio sources. Along these lines, there is a hole in the middle of this diffuse emission at $\alpha = 17^h11^m47^s.8$, $\delta = 64°09'52''$. The central diffuse emission on this image has a diameter of 500–600 kpc, which is less than 50% of the size of the Coma halo and is comparable to that seen around 3C 84 in the Perseus cluster (Burns et al. 1992). The flux density and power of this feature at 20 cm are 35 mJy and 4.7×10^{23} W Hz^{-1}, respectively. Interestingly, the tail associated with 1712+641 makes a sharp $\approx 90°$ bend to the NW at the position of the X-ray peak as it feeds into the diffuse radio emission. The entire diffuse emission bends away to the NW of the cluster X-ray centroid. The irregular shape and orientation make the diffuse radio emission in A2255 considerably different from the larger, symmetrical halo in Coma. Since the nature of the radio emission in A2255 is unclear, we will refer to this structure from here on as the "diffuse source."

Second, there is a peculiar, resolved ridge of radio emission to the NE of the cluster center ($\alpha = 17^h12^m46^s.3$, $\delta = 64°18'08''$). Because of its low surface brightness, the ridge was not seen on previous WSRT maps, but now appears on the higher contrast VLA image. It is ~ 500 kpc in extent. It makes a significant

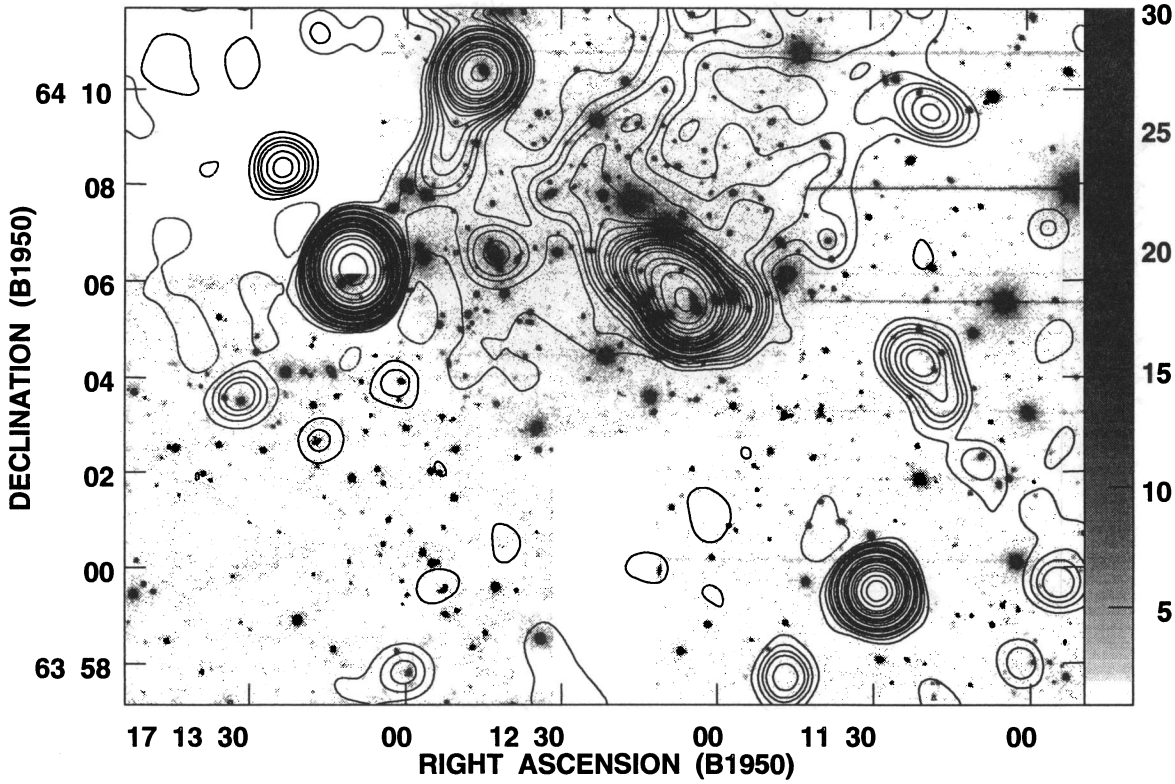

FIG. 5a

FIG. 5.—(*a*) Overlay of 20 cm radio contours onto the *r*-band CCD gray-scale image of A2255. The radio map has been convolved with a 50″ Gaussian beam. Note that the second contour at $\alpha = 17^h11^m47^s.8$, $\delta = 64°09'52''$ is actually a hole in the radio emission. Contour levels are $-1, 1, 2, 3, 4, 6, 8, 10, 15, 20, 25, 30, 40, 50, 60, 80, 100, 150, 200, 300$, and 500×0.3 mJy beam^{-1}. (*b*) Overlay of 20 cm radio contours onto the RASS gray-scale X-ray image of A2255. Gray scale ranges from 4.0×10^{-5} to 5.5×10^{-4} counts s^{-1} (15″ × 15″ pixel)$^{-1}$. Contour levels are the same as in Fig. 5*a*.

contribution to the halo flux density ($S_{20} = 18$ mJy; $P_{20} = 2.4 \times 10^{23}$ W Hz^{-1}). We overlaid the radio image into a *V*-band optical image of the cluster (not shown) from the STScI Guide Star plate archives and could not find any obvious optical ID or galaxy grouping in the vicinity of the ridge.

Third, the other two outlying head-tail sources in Figure 5*b* (1712+638 and 1714+641) are beyond the extent of the X-ray emission seen on the RASS map. These radio galaxies are confirmed members of the A2255 cluster (Harris et al. 1980). Models of head-tail radio galaxies (e.g., Jones & Owen 1979) require interaction of the radio plasma with the ICM via ram pressure and so suggest that there is substantial cluster gas that exists beyond that currently mapped by the RASS (Hintzen & Scott 1980).

Further discussion of the radio properties of A2255 at 20 and 90 cm will be presented in a future paper.

3. ANALYSIS OF CLUSTER PROPERTIES

3.1. *X-Ray Luminosity and ICM Temperature*

Edge & Stewart (1991a) and David et al. (1993) have most recently examined the relationship between cluster X-ray luminosity and ICM temperatures. Edge & Stewart find a strong correlation between bolometric X-ray luminosities and gas temperatures measured from observations with the *EXOSAT* telescope. They note, however, that there is significant scatter in the relationship which is beyond that produced by the measurement errors. Edge & Stewart attribute this to variations in the central densities between clusters. Similarly, David et al. find a correlation between temperature, measured from *Einstein* MPC spectra, and 2–10 keV luminosity in the form $kT = 10^{-0.59\pm0.02} L_x^{0.290\pm0.004}$ (1 σ errors) where kT is in keV and L_x is in units of 10^{40} ergs s^{-1}. Once again, there is considerable scatter within this strong correlation. For A2255, this relationship predicts a temperature of 6 keV; David et al. measured 7.3 keV.

3.2. *ICM Temperature and Cluster Velocity Dispersion*

Lubin & Bahcall (1993) recently re-examined the well-known relationship between gas temperature and galaxy velocity dispersion in clusters. Using measurements gathered from the literature with a variety of X-ray detectors, they found a correlation in the form $\sigma_R = 10^{2.52\pm0.07}(kT)^{0.60\pm0.11}$ (1 σ errors), where σ_R is in km s^{-1} and kT is in keV. Using the David et al. (1993) value of $kT = 7.3$ keV, this relationship predicts a velocity dispersion of 1091 km s^{-1} for A2255. Given the errors in σ_R and T, and the scatter in the above relationship, the measured value of σ_R (1208 km s^{-1}) is not significantly different from the predicted value. However, we note here that a value of σ_R ($\approx$1000 km s^{-1}) was needed in the X-ray profile deprojection to produce a temperature distribution consistent with the RASS and *Einstein* MPC spectral measurements (§ 2.1).

3.3. *Gas and Total Cluster Masses*

Next, we calculated the distribution of masses in A2255 using the X-ray and galaxy velocity data. In Figure 6*a*, the ICM mass distribution is shown which was computed by integrating the deprojected ICM density in Figure 2 within spher-

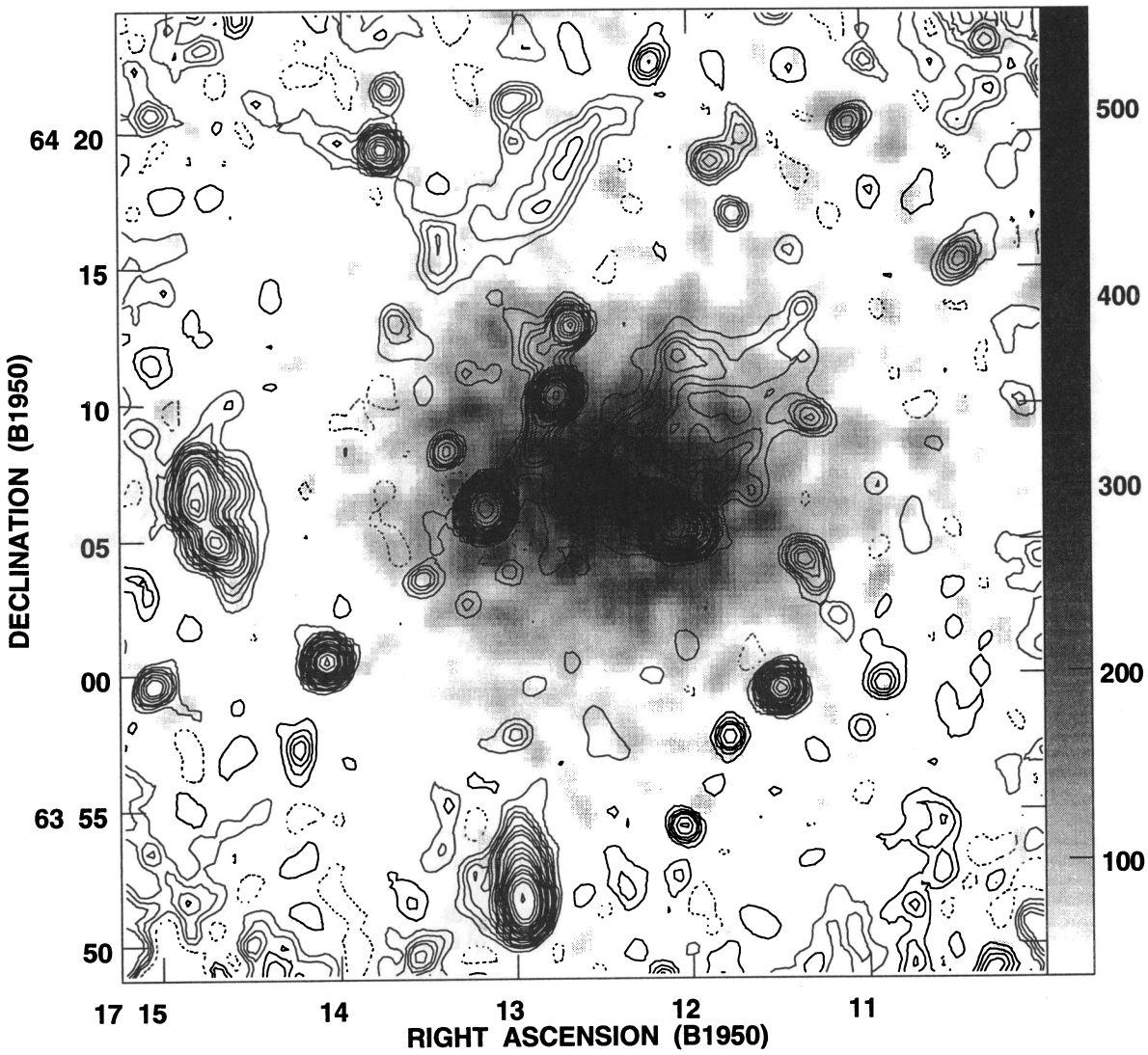

FIG. 5*b*

ical shells. In Figure 6*b*, the total mass distribution of the cluster is illustrated. This assumes that the gas is in hydrostatic equilibrium (which will be examined further in § 4) and is bound to the cluster gravitational potential (see, e.g., Sarazin 1986) such that

$$M(r) = -\frac{kT}{G\mu m_p}\left[\frac{d(\ln \rho)}{d(\ln r)} + \frac{d(\ln T)}{d(\ln r)}\right] r \,. \quad (1)$$

The gas mass within 0.8 Mpc of the cluster center is 2.6×10^{13} $M_\odot$ and the ratio of X-ray luminous to total mass at this radius is $\sim$6%. We see no evidence for an increase in the baryon fraction with distance from the cluster center in A2255. The average baryonic to dark matter ratio in A2255 is consistent with that measured for other rich clusters (see, e.g., Edge & Stewart 1991b).

We also calculated the dynamical mass in A2255 using the currently available galaxy positions and velocities. Using the Virial Theorem and assuming spherical symmetry, the total cluster dynamical mass is given by

$$M_{\rm VT} = \frac{3\pi}{G}\,\sigma_R^2 \left\langle \frac{1}{r} \right\rangle^{-1} , \quad (2)$$

where $\langle 1/r \rangle^{-1}$ is the harmonic mean radius (see, e.g., Oegerle & Hill 1994) and σ_R is the radial velocity dispersion. Using the biweight estimate of scale for σ_R, the Virial Theorem mass for A2255 is 1.2×10^{15} $M_\odot$. It should be noted that $M_{\rm VT}$ is the entire cluster mass, whereas $M(r)$ in equation (1) is calculated only out to 0.8 Mpc. These gas and total mass estimates are comparable to those found for the Coma cluster (Hughes 1989).

3.4. *ICM Gas Pressure and Radio Source Confinement*

We calculated the minimum pressure parameters for the diffuse radio emission in the cluster using the expressions in Burns, Owen, & Rudnick (1979) (with a corrected pressure equation). We assumed that the relativistic electrons and protons had equal energies, that the radio plasma filled the emitting volume, and that the *B*-field was transverse to the line of sight. The radio spectrum was assumed to extend in a power law from 10 MHz to 100 GHz with a spectral index of 1.7 (estimated from our 1.4 GHz image and a preliminary 0.33 GHz VLA image; see also Harris et al. 1980). We calculated the parameters for a cylindrical volume with the cylinder area given by the clean beam area and the length (assumed) equal to

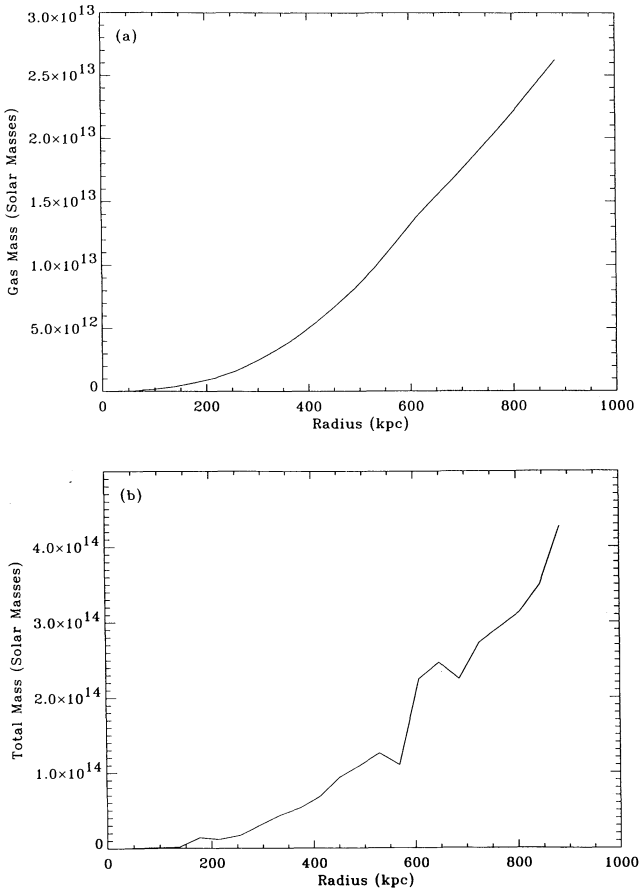

FIG. 6.—(*a*) Distribution of ICM gas mass calculated by summing the deprojected gas density in Fig. 2*a* within spherical shells. (*b*) Distribution of total (dark) mass in A2255 assuming the X-ray gas is in hydrostatic equilibrium and confined by the cluster potential.

the transverse width of the radio component. The results of these calculations are given in Table 2.

The estimated plasma pressure for the radio components ($\approx 8 \times 10^{-14}$ dyn cm^{-2}) is much less than the thermal pressure of the ICM estimated from the X-rays. Using the deprojected densities and temperatures in Figures 2*a* and 2*b*, we calculate that the ICM thermal pressure at distances of 400–800 kpc from the cluster center is $1\text{–}0.5 \times 10^{-11}$ dyn cm^{-2}. Similar underpressured cluster radio sources have been reported for Hydra A (Taylor et al. 1990), 1253+275 in the Coma-A1367 supercluster bridge (Giovannini, Feretti, & Stanghellini 1991), and a sample of tailed radio sources in Abell clusters (Feretti, Perola, & Fanti 1992).

3.5. *Central X-Ray Cooling Time*

The thermal (bremsstrahlung + lines) cooling time of the cluster core is approximately given by (Sarazin 1986)

$$\tau_{\rm cool} = 8.5 \times 10^{10} \left(\frac{n_e}{10^{-3}\ {\rm cm}^{-3}}\right)^{-1} \left(\frac{T}{10^8\ {\rm K}}\right)^{1/2} {\rm yr}\ . \quad (3)$$

From the deprojected gas density (2.2×10^{-3} cm^{-3}) and the central X-ray temperature (2.2×10^7 K) measured from the RASS spectrum, the cooling time at the center of A2255 is 1.8×10^{10} yr, which is about the Hubble time.

4. A CLUSTER/GROUP MERGER MODEL FOR A2255

Previous data and our new observations have revealed an interesting diversity of unusual properties for A2255. They include (1) the appearance of unusual, red compact galaxies, as defined by Zwicky (1971), throughout the cluster. (2) The cluster biweight scale (velocity dispersion) is very large ($\approx$1240 km s^{-1}). Also, the two brightest galaxies in this cluster are separated by 2635 km s^{-1}, with one of these galaxies in the low-velocity end of the cluster galaxy velocity distribution. The velocity dispersion for A2255 is larger than that needed to produce a gas temperature distribution, from a deprojection of the X-ray surface brightness distribution, that is consistent with the spectroscopically determined X-ray temperatures. (3) The X-ray peak, as imaged by both *Einstein* and *ROSAT* does *not* coincide with any bright cluster galaxies or any apparent subcluster. There is an elongation in the X-ray emission within the core of the cluster. Furthermore, the X-ray surface brightness profile is complex and not well fitted by a simple isothermal King model. (4) The central X-ray cooling time is about a Hubble time, yet RASS spectra indicate $T \approx 2$ keV in the core in contrast to the average cluster temperature of 7 keV. (5) Unusual diffuse radio structures were imaged by our new VLA 20 cm observations of A2255. A number of radio tails appear to merge together and form an extended, steep-spectrum diffuse source which bends away to the NW of the cluster center. About 0.6 Mpc from the cluster center, a curious, well-resolved ridge of radio emission also appears.

We believe that these properties can be understood if A2255 is currently in the process of merging with a smaller group of galaxies. To quantify this idea, we have run a cluster/subcluster merger simulation using the hybrid Hydro/*N*-Body code described by Roettiger, Burns, & Loken (1993). This code allows us to simulate the evolution of the ICM and its X-ray emission along with cluster dark matter during a merger. Our goal in this simulation was to determine if the general characteristics of A2255 could be understood within the context of a merger using the assumptions and physics inherent in our code.

TABLE 2

RADIO SOURCE PARAMETERS

Component	α(1950)	δ(1950)	D_c	$B_{\rm mp}$	$P_{\rm mp}$	$t_{\rm mp}$
Diffuse source.....	17^{h}11^{m}48^s	64°07′45″	410	0.91	7.7×10^{-14}	1.4×10^7
Diffuse source.....	17 11 36	64 11 29	460	0.91	7.6×10^{-14}	1.4×10^7
Ridge.....	17 12 52	64 17 15	625	0.93	8.0×10^{-14}	1.4×10^7

NOTES.—D_c is the projected distance of the radio component from the X-ray centroid in kiloparsecs. $B_{\rm mp}$ is the minimum pressure magnetic field in microgauss. $P_{\rm mp}$ is the minimum total (relativistic particles + B fields) pressure in dyn cm^{-2}. $t_{\rm mp}$ is the relativistic electron radiative lifetime due to synchrotron losses and inverse Compton scattering off of the microwave background in years.

In brief, our Hydro/*N*-body simulation used a combination of an Eulerian, finite-difference code called ZEUS-3D (Clarke 1990; Stone & Norman 1992) to evolve the cluster gas, and the Hernquist (1987) Treecode to evolve the gravitational potential. Thus, the gas responds to changes in both the gravitational and hydrodynamic (e.g., shocks and turbulence) forces on the grid. These hydrodynamic forces are quite important in determining the distribution of gas density, temperature, and X-ray emissivity during the merger. The hydro grid resolution was 50 kpc in the central 2 Mpc but gradually decreased outward. The simulation that we describe here is the same that was used to model the Coma/NGC 4839 cluster/group merger (Burns et al. 1994a). It is part of a broader parameter space study to investigate the effects of differing initial conditions on cluster mergers and cluster X-ray properties (Roettiger et al. 1995).

The simulations began with a head-on collision between two isothermal King spheres which were separated by 4 Mpc. The clusters had an initial relative infall velocity of 200 km s^{-1}. The masses of the clusters were 10^{15} $M_{\odot}$ (modeled with 18,000 particles) and 1.25×10^{14} $M_{\odot}$ (modeled with 2250 particles) for the rich and poor clusters, respectively. The initial temperature of the rich cluster was 7.2 keV and that of the poor group was 2.35 keV. The central density for each cluster was 2×10^{-3} cm^{-3}. The core radii were 250 kpc and 125 kpc. In both clusters, the gas mass was less than 10% of the total mass. The initial one-dimensional rms peculiar velocities were scaled to 930 km s^{-1} for the rich cluster and 450 km s^{-1} for the poor cluster. From the density and temperature distributions, we constructed synthetic X-ray images over the *ROSAT* band as described by Roettiger et al. (1993).

We recognize that the above parameters may not be completely optimized for A2255, but they are close enough to produce some additional physical insight into the plausibility of A2255 as a merger system. We examined the X-ray surface brightness and dark matter velocity distributions for different epochs (over an interval ± 0.3 Gyr of having the cluster cores coincide) and different merger axis projections (0°–50° to the line of sight). We found that the closest correspondence to A2255 occurred at a time of ≈ 0.13 Gyr after the cores were coincident and the merger axis oriented $\approx 30°$ to the line of sight. In Figure 7, the X-ray surface brightness and the distribution of projected radial velocities for the model are shown at this epoch.

There is generally good agreement between the X-ray image of A2255 in Figure 1 and the model X-ray image in Figure 7*a*, as well as, between the A2255 galaxy and model velocity distributions in Figure 7*b*. Both X-ray images reveal an elongation in the core which, in the model, is caused by gas that has not yet reached hydrostatic equilibrium within the gravitational potential well. In the model, the gas in the core is initially heated (to a peak of 8.5 keV) by shocks and then the temperature declines again as the core expands. Also, the distribution of particle velocities in the model agrees well with that in A2255. A χ^2 test demonstrates that the velocity histograms for A2255 and the model in Figure 7 agree at the 96% level. At the epoch shown in Figure 7, the two clusters have a relative velocity of ≈ 2450 km s^{-1}, comparable to the velocity difference of the brightest ellipticals in A2255.

The above merger model can help us to explain many of the peculiar properties of A2255. First, Zwicky's red compact galaxies are still not well understood. However, they might result from the interaction of galaxies in the poor group with those in the rich cluster or from ram pressure stripping by the ICM producing truncated star formation. Such cluster/subcluster mergers may explain the peculiar spectrum galaxies in the Coma/NGC 4839 cluster bridge (Burns et al. 1994a; Caldwell et al. 1994) and the Butcher & Oemler (1978) galaxies in more distant cluster galaxies. But, more optical work, particularly spectroscopy, is needed on these peculiar, compact galaxies in A2255 to determine their nature.

Second, the large dispersion in the galaxy velocity distribution in A2255 is expected if two subclusters are still undergoing a merger and have not yet relaxed. The large observed velocity

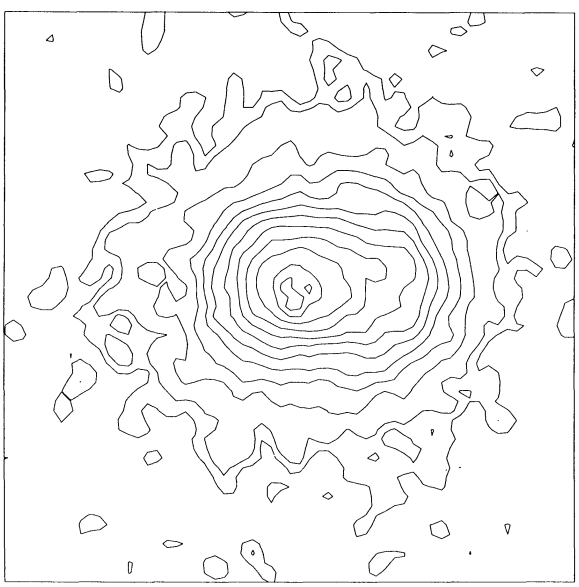

FIG. 7*a*

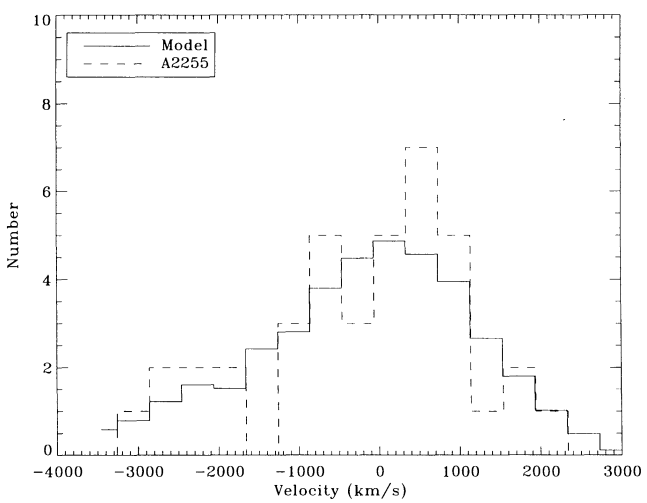

FIG. 7*b*

FIG. 7.—(*a*) Contours of X-ray emission for the merger model at 0.13 Gyr following the coincidence of the rich and poor cluster cores. Contour levels are 5.7%, 9.4%, 18.8%, 28.3%, 37.7%, 47.2%, 56.6%, 66.0%, 75.5%, 85.0%, 94.3%, and 99.0% of the peak. (*b*) Comparison of the distributions of relative velocities for galaxies in A2255 and particles in the merger model at the same epoch as that in (*a*).

difference between the brightest two elliptical galaxies in A2255 may suggest that one originates in the rich cluster, whereas the other is part of the merging group.

Third, the X-ray peak in A2255 may not coincide with the optical peak in the galaxy distribution because the ICM is not in hydrostatic equilibrium. The gas is streaming through the cluster center responding to the changes in the gravitational potential well and to shocks in the ICM.

Fourth, our model does not show any cool gas in the merged cluster center unlike that in A2255. This may suggest that A2255 had a preexisting cooling inflow which was not included in our simulation. The model suggests that shock-heating in the core during the merger may reduce the effective cooling producing a more modest inflow, relative to clusters like Perseus which have greater than 100 $M_\odot$ yr^{-1} accretion. Alternatively, the poor group may have deposited enough cold gas into the rich cluster core to stimulate the formation of a weak cooling flow (Fabian & Daines 1991). Furthermore, the lack of a galaxy or other optical emission at the X-ray centroid may be caused by the changing cluster gas environment. There may not have been enough time for gas to collect at the present X-ray centroid following the merger.

Fifth, the diffuse, steep-spectrum radio sources in A2255 may have been fueled by the merger of the clusters. As discussed in Burns et al. (1994a, b) and Tribble (1993), a strong correlation between X-ray substructure and steep-spectrum radio halos in clusters is beginning to emerge. The kinetic energy of the merger may fuel the in situ particle acceleration (via shocks or turbulence, e.g., Eilek & Hughes 1990) and the magnetic field amplification (e.g., De Young 1980) that is needed to maintain the extended radio emission. The coalescing galaxy group in our numerical simulation has a kinetic power of $\pi R_G^2 \rho_{\rm ICM} v_{\rm rel}^3 \sim 10^{46}$ ergs s^{-1} at the epoch of Figure 7, where R_G is the group radius (125 kpc), $\rho_{\rm ICM}$ is the ICM density (2×10^{-3} cm^{-3}), and $v_{\rm rel}$ is the relative velocity between the clusters (2450 km s^{-1}). This is sufficient to power the diffuse radio emission in A2255, which has a luminosity of 3×10^{41} ergs s^{-1} (assuming a continuous power-law spectrum with $\alpha = 1.7$ between 10 MHz and 100 GHz), with a modest conversion efficiency. Bulk gas motions in the ICM produced by the merger (Roettiger et al. 1993; Schindler & Müller 1993) may also sweep the diffuse emission away from the core to the NW.

We conclude by noting that if the above model is correct, A2255 is far from Virial and hydrostatic equilibrium. Therefore, the masses calculated in § 3.3 may have large errors.

5. SUMMARY AND CONCLUSIONS

A2255 has a number of unusual properties, which make it unlikely that the cluster is a simple relaxed system; the galaxies and dark matter are probably not in Virial equilibrium nor is the ICM in hydrostatic equilibrium. These unusual properties include the appearance of red compact galaxies throughout the cluster, a very high galaxy velocity dispersion (1240 km s^{-1}), an X-ray cluster centroid which does not coincide with either the brightest cluster galaxies or any obvious subcluster, a large X-ray core radius (> 500 kpc), possible cool gas in the core (2 keV) in comparison to the cluster average (7 keV), and diffuse, steep-spectrum, radio emission distributed nonuniformly within the cluster. Using new Hydro/N-body simulations, we can explain most of these properties if A2255 is in the process of undergoing a merger with a group of galaxies.

There is a commonality in the properties of the three best examples of Jones & Forman's (1982) class nXD clusters—Coma (Burns et al. 1994a), A2255, and A2256 (Briel et al. 1991; Röttgering et al. 1994). These clusters all exhibit evidence of X-ray substructure, do not have high-mass flux central cooling flows, but do have high-velocity dispersions, hot ICMs, and steep-spectrum, diffuse radio sources. A picture of this class of cluster as systems which are in the process of merging is beginning to take shape.

Additional redshift measurements for A2255 are needed to better constrain the galaxy velocity distribution and to search for substructure. Also, multicolor and Hα imaging, and spectroscopic observations in A2255 would be useful to determine the nature of the peculiar red compact galaxies. Similar multiwavelength observations of other nXD and radio halo clusters should provide additional tests of the above model and insight into the nature of this class of cluster.

This work was partially supported by a NASA Long Term Space Astrophysics grant NAGW-3152 to JOB and FNO, and an NSF grant AST-9317596 to JOB. KR was also partially supported by a New Mexico NASA Space Grant Consortium fellowship, and JP by a Sigma Xi grant-in-fellowship. We thank Dan Harris for his extensive comments on the text, M. Ledlow for his help with the minimum pressure calculations, Bill Oegerle for the "quick V" image of A2255, NOAO for the IRAF package, NRAO for AIPS, CfA for PROS, and MPE for EXSAS. JOB and FNO also thank MPE and its director, J. Trümper, for their hospitality during the initial stages of this research. ZEUS-3D is maintained by the Laboratory for Computational Astrophysics at NCSA.

REFERENCES

Abell, G. O. 1958, ApJS, 3, 211
Abell, G. O., Corwin, H. G., & Olowin, R. P. 1989, ApJS, 70, 1
Arnaud, K. A. 1988, in Cooling Flows in Clusters and Galaxies, ed. A. C. Fabian (Dordrecht: Kluwer), 31
Bautz, L., & Morgan, W. 1970, ApJ, 162, L149
Beers, T. C., Flynn, K., & Gebhardt, K. 1990, AJ, 100, 32
Bird, C. M., & Beers, T. C. 1993, AJ, 105, 1586
Briel, U., et al. 1991, A&A, 246, L10
Burns, J. O., Owen, F. N., & Rudnick, L. 1979, AJ, 84, 1683
Burns, J. O., Roettiger, K., Ledlow, M., & Klypin, A. 1994a, ApJ, 427, L87
Burns, J., Roettiger, K., Pinkney, J., Loken, C., Doe, S., Owen, F., Voges, W., & White, R. 1994b, in The Soft X-Ray Cosmos, ed. E. M. Schlegel & R. Petre (New Yorks: AIP), 183
Burns, J. O., Sulkanen, M. E., Gisler, G. R., & Perley, R. A. 1992, ApJ, 388, L49
Butcher, H., & Oemler, A. 1978, ApJ, 219, 18
Butcher, J. A., & Stewart, G. C. 1991, in NATO Advanced Study Institute, Clusters & Superclusters of Galaxies, ed. M. M. Colless, A. Babul, A. C. Edge, R. M. Johnstone, & S. Raychaudhury (Dordrecht: Kluwer), 25
Caldwell, N., Rose, J. A., Sharples, R. M., Ellis, R. S., & Bower, R. G. 1993, AJ, 106, 473
Clarke, D. A. 1990, BAAS, 22, 1302
Danese, L., DeZotti, G., & di Tullio, G. 1980, A&A, 82, 322
David, L. P., Slyz, A., Jones, C., Forman, W., Vrtilek, S. D., & Arnaud, K. A. 1993, ApJ, 412, 479
De Young, D. S. 1980, ApJ, 241, 81
Dressler, A., & Shectman, S. A. 1988, AJ, 95, 985
Edge, A. C., & Stewart, G. C. 1991a, MNRAS, 252, 414
———. 1991b, MNRAS, 252, 428
Edge, A. C., Stewart, G. C., & Fabian, A. C. 1992, MNRAS, 258, 177
Eilek, J. A., & Hughes, P. E. 1990 in Astrophysical Jets, ed. P. E. Hughes (Cambridge: Cambridge Univ. Press), 428
Fabian, A. C., & Daines, S. J. 1991, MNRAS, 252, 17p
Feretti, L., Perola, G. C., & Fanti, R. 1992, A&A, 265, 9
Forman, W., & Jones, C. 1982, ARA&A, 20, 547
Giovannini, G., Feretti, L., & Stanghellini, C. 1991, A&A, 252, 528
Hanisch, R. J. 1982, A&A, 116, 137
Harris, D. E., Kapahi, V. K., & Ekers, R. D. 1980, A&AS, 39, 215
Harris, D. E., et al. 1990, The Einstein Observatory Catalog of IPC X-Ray Sources (Washington, DC: Smithsonian Astrophysical Observatory)
Hernquist, L. 1987, ApJS, 64, 715

Hintzen, P., & Scott, J. S. 1980, ApJ, 239, 765
Hughes, J. P. 1989, ApJ, 337, 21
Jaffe, W. J., & Rudnick, L. 1979, ApJ, 233, 453
Jones, C., & Forman, W. 1984, ApJ, 276, 38
Jones, T. W., & Owen, F. N. 1979, ApJ, 234, 818
Kowalski, M. P., Ulmer, M. P., Cruddace, R. G., & Wood, K. S. 1984, ApJS, 56, 403
Lubin, L. M., & Bahcall, N. A. 1993, ApJ, 415, L17
McMillan, S. L. W., Kowalski, M. P., & Ulmer, M. P. 1989, ApJS, 70, 723
Oegerle, W. R., & Hill, J. M. 1994, AJ, 107, 857
Perley, R. A., Schwab, F. R., & Bridle, A. H., eds. 1989, Synthesis Imaging in Radio Astronomy, Vol. 6 (San Francisco: ASP)
Raymond, J. C., & Smith, B. W. 1977, ApJS, 35, 419
Rhee, G., van Haarlem, M., & Katgert, P. 1992, AJ, 103, 1721
Roettiger, K., Burns, J. O., & Loken, C. 1993, ApJ, 407, L53
Roettiger, K., Loken, C., & Burns, J. O. 1995, ApJS, submitted
Röttgering, H., Snellen, I., Miley, G., de Jong, J. P., Hanisch, R., & Perley, R. 1994, ApJ, 436, 654
Sarazin, C. L. 1986, Rev. Mod. Phys., 58, 1
Schindler, S., & Müller, E. 1993, A&A, 272, 137
Stark, A. A., Gammie, C. F., Wilson, R. W., Bally, J., Linke, R. A., Heiles, C., & Hurwitz, 1992, ApJS, 79, 77
Stauffer, J., Spinrad, H., & Sargent, W. L. W. 1979, ApJ, 228, 379
Stewart, G. C., Fabian, A. C., Jones, C., & Forman, W. 1984, ApJ, 285, 1
Stone, J., & Norman, M. 1992, ApJS, 80, 791
Tarenghi, M., & Scott, J. S. 1976, ApJ, 207, L9
Taylor, G. B., Perley, R. A., Inoue, M., Kato, T., Tabara, H., & Aizu, K. 1990, ApJ, 360, 41
Thuan, T. X., & Gunn, J. E. 1976, PASP, 88, 543
Tribble, P. C. 1993, MNRAS, 263, 31
Trümper, J. 1993, Science, 260, 1769
Ulmer, M. P., Wirth, G. D., & Kowalski, M. P. 1992, ApJ, 397, 430
Voges, W. 1992, in Proc. European "International Space Year" Conf., ESA ISY3, ed. T. D. Guyenne & J. J. Hunt (Noordwijk: ESA), 9
Zwicky, F. 1971, Catalogue of Selected Compact Galaxies & of Post-Eruptive Galaxies (Zurich: Offsetdruck L. Speich)
Zwicky, F., & Herzog, E. 1986, Catalog of Galaxies & of Clusters of Galaxies, Vol. IV (Pasadena: California Inst. of Technology), 140